Supporting Information

Liu *et al.* 10.1073/pnas.0807007105

SI Text

Further Assumptions on the Mechanobiochemical Feedback Mechanism

1. Right after the other spindle pole captures unattached kinetochore of monooriented chromosome, the number of kinetochore microtubules (KMTs) attaching to each sister chromatid might be different initially. Consequently, the traction forces from each side of the chromosome might tend to be different. During the ensuing movement of the forming bioriented chromosome, more microtubules would attach to the newly captured kinetochore shortly; hence, the number of KMTs from both sides of the bioriented chromosome will eventually be equal in a short period. Our model does not explicitly account for such a detailed process of changing KMTs; strictly speaking, it therefore will account only for the scenario that the sister chromatids possess an equal number of KMTs. However, as we have demonstrated in the main article, the mechanical force impinging on the chromosome is in a closed feedback with the local chemical reactions, the difference in the number of KMTs during the initial period of biorientation formation of the chromosome would have a similar effect as the inequality in the chemical states between the sister chromatids (i.e., the local levels of R_i, R_i^*, and S_i). Also, regardless of the inequality in the initial chemical states between sister chromatids, our model can always recapitulate the essential features of the sequential changes in the chromosome motility throughout mitosis. Therefore, we believe that the general features for the bioriented chromosome motility predicted by our model will still be valid, even though the model does not explicitly account for the initial inequality in the KMT numbers from both sides of the chromosome. Furthermore, the chromosome movement requires the dynamics of the multiple KMTs at the same kinetochore to be synchronized. In the model, we assume that such synchronization is instantaneous such that there is no time delay in chromosome movement.
2. For Eq. **1** in the main text, chromatid velocity is the product of the mechanical (the velocity constant V_i) and chemical (the local active regulator level R_i^*) factors. Here, V_i represents the intrinsic strength of the proteins and/or microtubule itself in controlling the growth and shrinkage of the microtubule spindle plus end. In the model, V_i does not explicitly have load-force dependence, which could have at least two interpretations. First, it is appropriate if the effective motor activity, including polymerizing and depolymerizing microtubule plus end, is insensitive to load force (namely, the plateau region of the velocity vs. load-force plot). When many motor proteins work in synergy, which is surely the case for chromokinesins, this "load-force-insensitive" range could become very large and cover the typical range of mechanical force that chromosome encounters during mitosis. Consequently, V_i could be independent of load force. Second, because the entire system of chromosome motility is a mechanochemical-coupled system, any effect of the load force on the chromosome can, in principle, reflect on the local chemical state, which will ultimately change R_i^*. This, in turn, will modulate the effective chromatid velocity. The velocity constant V_i in this scenario can be interpreted as the activation rate of the motor proteins that directly govern chromosome velocity. Also, the hidden assumption here is that the availability of the motor proteins at the plus end of the microtubule is not changed by load force. Note that the apparent chromatid velocity may be much more complicated than $V_i(R_i^* - R_0)$. We stress that we want to start from the simplest scenario to illustrate the basic physical factors, which is also in accordance with the experimental observation that the chromosome motility correlates with its local kinase level at kinetochore. We also will leave the study of more complicated situations to future investigations.
3. The "sensor" in the model is actually one identity that could consist of many proteins. This stable identity could be a physically linked protein scaffold complex, such as the MCC complex (1–3), or it could consist of several different proteins (4) (e.g., the mitotic checkpoint proteins, polo-like kinase, and MAPK) such that the intrinsic recruitment reactions among these proteins may take place at much faster time scale than all of the other reactions in the model. Consequently, in the time scale of chromosome oscillation, the dynamics of these subsets of the proteins could be collectively and effectively represented by one identity. Also, we did not specify such details and complications in our model.
4. The AP force spatial gradient $|\alpha|$ is, in fact, the effective force gradient, stemming from several sources: (*i*) The spare microtubules emanating from spindle poles (non-KMT) polymerize and could "push" the chromosome arms (5). Because they are sparse close to the cell equator and highly condensed near the spindle pole because of their astral formation (5), the effective AP force by these spare microtubules tends to form an increasing gradient toward the spindle pole. (*ii*) The chromokinesin motor proteins that bind to KMTs and the non-KMTs push the chromosome in the AP directions. Because the density of the chromokinesins correlates with that of the microtubules, its effective AP force will also exhibit the same spatial gradient (5, 6). Note that the chromokinesin can exert the AP force only when it binds to chromosome, which depends on the Cdk/cyclin B kinase activation (7–12). This corresponds to the R^*-dependent term in Eq. **4**. (*iii*) Certain depolymerase motor proteins that concentrate on the plus end of KMT form a decreasing gradient toward the spindle pole (13, 14). Because these depolymerases induce shrinkage of the KMT plus end, they provide a poleward driving force for the chromosome. Therefore, a decreasing gradient in the P force will effectively reflect on an increasing gradient in the AP force.
5. The kinetochore resistance in the model essentially stems from the mechanical stretch of chromosome, which reflects on the elastic stress in the kinetochore region and along the chromosome arms. It is not entirely clear how this sensor protein responds to such mechanical stress at the molecular level (15). In the model, we simply incorporated the output of the response between kinetochore resistance and sensor protein level and leave the further exploration of the molecular mechanism for such response to future study.

Now we derive the explicit formula for the local kinetochore resistance $\Gamma(x, t)$, and we focus on only one chromatid here. The kinetochore resistance is increased by the AP ejection force modulated by the chromosome position and the regulator R^* activation and is further affected by the viscous drag on the chromosome. This effect is captured by the equation

$$\Gamma = \underbrace{-\Gamma_1}_{\text{P force}} + \underbrace{(A + Bx)R^*}_{\text{AP force}} + \underbrace{\eta V}_{\text{Viscous drag}},$$

where Γ_1 is the P pulling force arising from KMT plus-end shrinkage, $(A + Bx)R^*$ is the AP force that is activated by R^*

and has an increasing poleward gradient ($A + Bx$), and ηV is the viscous drag from chromosome movement with η being the viscous drag coefficient. Because $V = V_0(R^* - R_0)$, the kinetochore resistance can be represented as $\Gamma = (A - \eta V_0)(\Gamma_0 + (1 + \alpha x)R^*)$, where

$$\Gamma_o = -\frac{\Gamma_1 \eta V_0 R_0}{A - \eta V_0}, \qquad \alpha = \frac{B}{A - \eta V_0}.$$

Γ_0 describes the residual kinetochore resistance arising from the intrinsic KMT plus-end shrinkage, and $(1 + \alpha x)$ describes the postulated space-dependent AP ejection force along the spindle axis, with $\alpha < 0$ for $x < 0$ and $\alpha = 0$ for $x > 0$. This form gives an increasing poleward profile that is taken as a fixed background field (i.e., it is assumed to be not perturbed by chromosome movement). Therefore, with the recruitment rate of the sensor S in Eq. **4**: $k_6(1 + \alpha x)R^*$, $(A - \eta V_0)$ is absorbed into k_6, and the remaining constant − the Γ_0 term is assumed to be cancelled out between sister chromatids. In the model, all of the inequalities between sister chromatids will be reflected in the initial conditions (i.e., different chromatid position, different local protein levels, etc).

6. The location of the cell equator is determined by the AP force spatial gradients $|\alpha|$ in the model, and the pinpointing of the chromosome at the cell equator naturally depends on the AP force gradient $|\alpha|$. Our model does not deal with the issues of what determines the specific configuration of the AP force gradients, which has to do with the detailed interactions between the cortical actin network and the microtubules (16), and we would explore these processes in the future. We can also show that the pinpointing chromosome to the cell equator is not affected by the variation of the configuration of the force gradient $|\alpha|$, including the asymmetry in the force gradients across the cell equator (data not shown). Therefore, the prediction of our model is insensitive to the specific α configuration.
7. To relate the concentration to the actual number of proteins, we assumed that the radius of our virtual cell is ≈16 μm, leading to volume ≈1.6×10^4 μm^3, which determines that 1 nM ≈ 1×10^4 molecules per cell. Moreover, the proteins involved are highly localized at the kinetochore region. Thus, the amounts of the proteins at each kinetochore region are roughly their total number in one cell divided by the number of kinetochores. If we assume that there are ≈10 chromosomes, which leads to 20 kinetochore regions, then 1 nM corresponds to ≈500 molecules per kinetochore region.
8. The synthesis rate of cyclin B in interphase is ≈1 nM/min (17, 18). During mitosis, the protein synthesis rate is generally reduced to 25–30% of that in interphase (19). Therefore, the cyclin B synthesis rate in mitosis $k_1 \approx 0.25 - 0.3$ nM·min^{-1}. As soon as the new cyclin B is produced, it will mainly distribute and localize at the centrosome, the spindle microtubule, and the kinetochore/chromosome region while leaving its pool in cytoplasm intact (20, 21). Consequently, the actual synthesis rate of cyclin B at each kinetochore region would be further reduced roughly by a factor of 2–3, according to refs. 20 and 21. Therefore, the cyclin B synthesis rate per kinetochore region in the model is estimated to be $k_1 \approx 0.1$ nM·min^{-1}, which corresponds to the situation that 50 more cyclin B molecules will appear at each kinetochore region per minute. (We emphasize that the exact values of the kinetic parameters in the model would not qualitatively change the phase diagram in the model.)
9. We lump the interconversions of Cdc2/cyclin B at different phosphorylation sites into only two reactions: (*i*) the bare cyclin B synthesis, which is far more abundant in mitosis (17, 18, 22–24) and, thus, binds to Cdc2 instantaneously, resulting in the bare and inactive Cdc2/cyclin B; and (*ii*) the conversion of the bare Cdc2/cyclin B into the active form. Such conversion dynamics largely favors the active Cdc2/cyclin B in mitosis, which is in part because the Cdc2/cyclin B inhibitory phosphorylation is predominantly prohibited by various pathways after prophase, such as those involving Polo-like kinase (25).
10. See Fig. S1.
11. In the model, we considered the motility of only a single chromosome while taking all of the other chromosomes in the same mitotic cell as background. We did not explicitly take into account the steric interactions among chromosomes. It is conceivable that a larger chromosome would experience more viscous drags and much more steric repulsions when it moves through the region where many other chromosomes are residing. Therefore, the intrinsic motility of the chromosome that is determined by the proposed mechanobiochemical feedback mechanism could be "slaved" by the external steric interactions among chromosomes. Thus, it follows that larger bioriented chromosome might not exhibit as vigorous oscillation as the smaller one does (26). Because the main focus in the article is to investigate the intrinsic feedback mechanism that governs chromosome motility in mitosis, we will leave the more complicated scenarios of interactions among chromosomes as well as chromosomes of different sizes to future work.

Consequence of Disassembly of the Mechanobiochemical Feedback at Improper Timing

See Fig. S2.

The Dependence of Bioriented Chromosome Oscillation

See Figs. S3 and S4.

For large velocity constant V_0 and large spatial gradient in AP force α, the feedback between the chromosome movement and the local chemical reaction is very potent, leading to the active regulator levels at both chromatids that are always higher than the threshold level R_0 (Fig. S4*A*). Consequently, the active regulators at both sides tend to push their own chromatid toward the cell equator (i.e., opposing instead of facilitating each other as compared to the case in Fig. 4*A* in the main text). Subsequently, the sister chromatids always bump into each other just like the tug-of-war, with a reduced interkinetochore distance that is balanced only by steric repulsion between the sister chromatids (Fig. S4*B*). Therefore, instead of synchronizing with each other, such tugs-of-war slow down the overall velocity of their mass center. In comparison, with a large velocity constant V_0 and a smaller spatial gradient in AP force α, the active regulator R^* for both sides always oscillate around R_0 (like those in Fig. 4*A*). As just demonstrated, the facilitating effect synchronizes and, hence, makes bioriented chromosome oscillation easier, leading to a faster oscillation velocity than that for the larger α. On the other hand, at a smaller velocity constant V_0 in Fig. 4*C*, the mechanobiochemical feedback is not potent anyway, and R^* will always maintain around R_0 anyway, regardless of how large or small the spatial gradient in AP force α is. In such cases, the sister chromatids will again move synchronously, facilitating each other like those in Fig. 4*A*. In such a scenario, a larger spatial gradient α imposes a relatively faster feedback (Eq. **4**), which will conceivably synchronize faster between the sister chromatids, resulting in a faster oscillation velocity than that for the smaller spatial gradient. In other words, it is the potency of the proposed feedback mechanism that affects the overall levels of the active regulator R^* and, hence, leads to the transition from a synchronizing effect ($R^* \approx R_0$) to antagonizing effect ($R^* > R_0$) between the movements of the sister chromatids. When the interaction between the sister chromatids is completely turned

off with each behaving just like the monooriented chromosome, there are no synchronizing or antagonizing effects at all. And, as Fig. S4*C* shows, the average oscillation velocity in this scenario is consistently larger for larger spatial gradient α for all range of the velocity constant V_0.

The predictions from our model (Fig. 4*C*) could reconcile the controversy of the bioriented chromosome motility change in the Kif18 mutant (32, 33), which can affect both the spatial gradient α in force and the velocity constant V_0. In these experiments, both increase and decrease in the average bioriented chromosome oscillation velocity have been observed when the Kif18 motor protein activity is turned off. According to the model, this could just be attributable to the different routes of Kif18 mutant effects, starting from the different initial conditions in Fig. 4*C*.

The Elastic Constant of Cohesion Between Sister Chromatids Does Not Qualitatively Affect the Characteristics of Bioriented Chromosome Motility

See Fig. S5.

Segregated Chromatids Can Undergo Dampened Oscillation

See Figs. S6 and S7.

Discussion of Chromosome Motility in Mitotic Yeast Cells

Now we take a small excursion to discuss the different chromosome motilities in yeast from those of mammalian cells in mitosis. The questions are: Why is there no sustained regular chromosome oscillation in yeast whereas there is in mammalian cells (34, 35)? And, can our model explain such a difference? In contrast to mammalian cells, yeast has "closed" mitosis (36) [i.e., the nuclear envelope never breaks down, which always confines the chromosomes within 1–2 μm in linear dimension as compared with $\approx$20 μm in mammalian cells (35)]. We conjecture that: (*i*) The small space in which the yeast chromosome resides makes it much easier to be captured by the spindle microtubule. Hence, functionally, it may not need the elaborate monooriented chromosome oscillation to enhance its chance of being captured. (*ii*) There are only a few spindle microtubules inside the yeast nuclear envelope, which cannot form any sizable spatial gradient of the AP ejection forces. Mechanistically, the yeast chromosome may not undergo significant stretching to invoke the tension-sensor protein and, hence, is not capable of sustained oscillation, as shown in our model (Fig. 3*B*). (*iii*) Yeast does not have the full mechanobiochemical feedback at the kinetochores because it does not have BubR1, which synergistically interacts with Mad2 to substantiate the full mitotic checkpoint activity [the checkpoint activity of Mad2 alone is $\approx$12 times weaker than that of the BubR1 and Mad2 combination (2) and 3,000 times weaker than that of the MCC complex in mammalian cells (1)]. Accordingly, the feedback strength K_C could be below the required threshold for chromosome oscillation (Fig. 3*C*). (*iv*) Instead of being determined by the kinetochores as in mammalian cells, the yeast chromosomes together with the nuclear envelope are positioned as a whole by the interaction between the spindles anchored at the cell cortex and spindle pole body (36, 37), the stochastic fluctuation of which could, in turn, lead to the variation in chromosome position. Overall, yeast seems to use a different mechanism of controlling chromosome motility in mitosis even though it has nearly all of the key proteins as in mammalian cells that control KMT plus-end dynamics, kinetochore tension sensing, and mitotic checkpoints (except BubR1). Therefore, it remains interesting to determine if the exquisite mechanobiochemical feedback mechanism could be of evolutionary advantage in mitoses that evolve from lower to higher eukaryotes.

1. Sudakin V, Chan GKT, Yen TJ (2001) Checkpoint inhibition of the APC/C in HeLa cells is mediated by a complex of BUBR1, BUB3, CDC20, and MAD2. *J Cell Biol* 154:925–936.
2. Fang GW (2002) Checkpoint protein BubR1 acts synergistically with Mad2 to inhibit anaphase-promoting complex. *Mol Biol Cell* 13:755–766.
3. Tang ZY, Bharadwaj R, Li B, Yu HT (2001) Mad2-independent inhibition of APC^{Cdc20} by the mitotic checkpoint protein BubR1. *Dev Cell* 1:227–237.
4. Liu ST, Rattner JB, Jablonski SA, Yen TJ (2006) Mapping the assembly pathways that specify formation of the trilaminar kinetochore plates in human cells. *J Cell Biol* 175:41–53.
5. Cassimeris L, Reider CL, Salmon ED (1994) Microtubule assembly and kinetochore directional instability in vertebrate monopolar spindles: Implications for the mechanism of chromosome congression. *J Cell Sci* 107:285–297.
6. Levesque AA, Compton DA (2001) The chromokinesin Kid is necessary for chromosome arm orientation and oscillation, but not congression, on mitotic spindles. *J Cell Biol* 154:1135–1146.
7. Andersen SSL, *et al*. (1997) Mitotic chromatin regulates phosphorylation of stathmin/Op18. *Nature* 389:640–643.
8. Budde PP, Kumagai A, Dunphy WG, Heald R (2001) Regulation of Op18 during spindle assembly in *Xenopus* eggs extracts. *J Cell Biol* 153:149–157.
9. Andrew PD, *et al*. (2004) Aurora B regulates MCAK at the mitotic centromere. *Dev Cell* 6:253–268.
10. Ohsugi M, *et al*. (2003) Cdc2-mediated phosphorylation of Kid controls its distribution to spindle and chromosomes. *EMBO J* 22:2091–2103.
11. Ruderman JV, Gadea BB (2006) Aurora B is required for mitotic chromatin-induced phosphorylation of Op18/Stathmin. *Proc Natl Acad Sci USA* 103:4493–4498.
12. Hyman AA, Mitchison TJ (1990) Modulation of microtubule stability by kinetochores in vitro. *J Cell Biol* 110:1607–1616.
13. Varga V, *et al*. (2006) Yeast kinesin-8 depolymerizes microtubules in a length-dependent manner. *Nat Cell Biol* 8:957–962.
14. Gupta MLJ, Carvalho P, Roof DM, Pellman D (2006) Plus end-specific depolymerase activity of Kip3, a kinesin-8 protein, explains its role in positioning the yeast mitotic spindle. *Nat Cell Biol* 8:913–923.
15. Doncic A, Ben-Jacob E, Barkai N (2005) Evaluating putative mechanisms of the mitotic spindle checkpoint. *Proc Natl Acad Sci USA* 102:6332–6337.
16. Lénárt P, *et al*. (2005) A contractile nuclear actin network drives chromosome congression in oocytes. *Nature* 436:812–818.
17. Kumagai A, Dunphy WG (1995) Control of the Cdc2/cyclin B complex in *Xenopus* egg extracts arrested at a G_2/M checkpoint with DNA synthesis inhibitors. *Mol Biol Cell* 6:199–213.
18. Lee TH, Turck C, Kirschner MK (1994) Inhibition of cdc2 activation by INH/PP2A. *Mol Biol Cell* 5:323–338.
19. Breton ML, Cormier P, Bellé R, Mulne-Lorillon O, Morales J (2005) Translational control during mitosis. *Biochimie* 87:805–811.
20. Huang JY, Raff JW (1999) The disappearance of cyclin B at the end of mitosis is regulated spatially in *Drosophila* cells. *EMBO J* 18:2184–2195.
21. Huang JY, Raff JW (2002) The dynamic localization of the *Drosophila* APC/C: Evidence for the existence of multiple complexes that perform distinct functions and are differentially localized. *J Cell Sci* 115:2847–2856.
22. Galas S, Barakat H, Doree M, Picard A (1993) A nuclear factor required for specific translation of cyclin B may control the timing of first meiotic cleavage in starfish oocytes. *Mol Biol Cell* 4:1295–1306.
23. Murray A, Kirshner MW (1989) Cyclin synthesis drives the early embryonic cell cycle. *Nature* 339:275–280.
24. Murray A, Solomon MJ, Kirschner MW (1989) The role of cyclin synthesis and degradation in the control of maturation promoting factor activity. *Nature* 339:280–285.
25. Qian YW, Erikson E, Li C, Maller JL (1998) Activated polo-like kinase Plx1 is required at multiple points during mitosis in *Xenopus laevis*. *Mol Cell Biol* 18:4262–4271.
26. Khodjakov A, Cole RW, McEwen BF, Buttle KF, Reider CL (1997) Chromosome fragments possessing only one kinetochore can congress to the spindle equator. *J Cell Biol* 136:229–240.
27. Howell BJ, *et al*. (2004) Spindle checkpoint protein dynamics at kinetochores in living cells. *Curr Biol* 14:953–964.
28. Shah JV, *et al*. (2004) Dynamics of centromere and kinetochore proteins: Implications for checkpoint signaling and silencing. *Curr Biol* 14:942–952.
29. Helenius J, Brouhard G, Kalaidzidis Y, Diez S, Howard J (2006) The depolymerizing kinesin MCAK uses lattice diffusion to rapidly target microtubule ends. *Nature* 441:115–119.
30. Emanuele MJ, McCleland ML, Satinover DL, Stukenberg PT (2005) Measuring the stoichiometry and physical interactions between components elucidates the architecture of the vertebrate kinetochore. *Mol Biol Cell* 16:4882–4892.
31. Kline-Smith SL, Khodjakov A, Hergert P, Walczak CE (2004) Depletion of centromeric MCAK leads to chromosome congression and segregation defects due to improper kinetochore attachments. *Mol Biol Cell* 15:1146–1159.
32. Mayr MI, *et al*. (2007) The human kinesin Kif18A is a motile microtubule depolymerase essential for chromosome congression. *Curr Biol* 17:488–498.
33. Stumpff J, von Dassow G, Wagenbach M, Asbury C, Wordeman L (2008) The kinesin-8 motor Kif18A suppresses kinetochore movements to control mitotic chromosome alignment. *Dev Cell* 14:252–262.
34. Gardner MK, *et al*. (2005) Tension-dependent regulation of microtubule dynamics at kinetochores can explain metaphase congression in yeast. *Mol Biol Cell* 16:3764–3775.
35. Skibbens RV, Skeen VP, Salmon ED (1993) Directional instability of kinetochore motility during chromosome congression and segregation in mitotic newt lung cells: A push-pull mechanism. *J Cell Biol* 122:859–875.

36. Huisman SM, Segal M (2005) Cortical capture of microtubules and spindle polarity in budding yeast: Where's the catch? *J Cell Sci* 118:463–471.
37. Zheng L, Schwartz C, Magidson V, Khodjakov A, Oliferenko S (2007) The spindle pole bodies facilitate nuclear envelope division during closed mitosis in fission yeast. *PLoS Biol* 5:1530–1542.

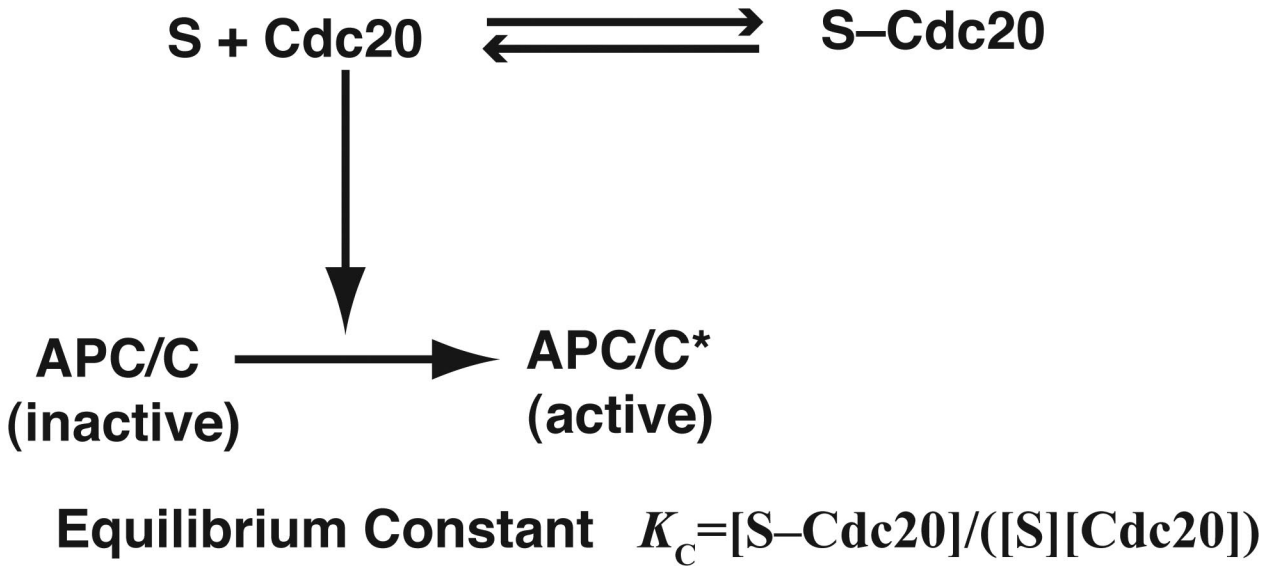

Fig. S1. Schematic of the conjugation reaction by which the ''sensor'' inhibits the degradation machinery. In the model, we assume that the conjugation between the sensor and Cdc20 instantaneously reaches equilibrium with the equilibrium constant K_C. Assuming the local total Cdc20 level ([Cdc20] + *S*–Cdc20]) is fixed such that conjugation attenuates the degradation rate k_4 by a factor of $(1 + K_C S)$.

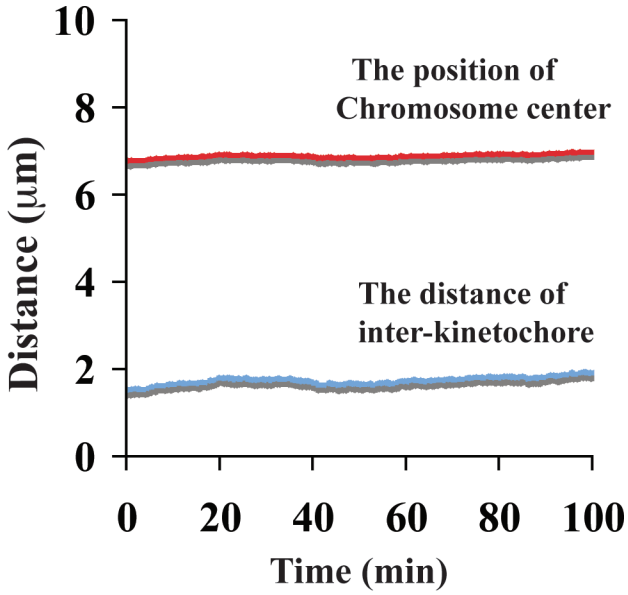

Fig. S2. The bioriented chromosome can be far away from the equator while maintaining the mechanical force balance and chemical balance from both sides, if the feedback between the mechanics and the chemistry is impaired [e.g., the feedback among *S*, *R*, and *R** is absent (k_3 and K_C are zero)].

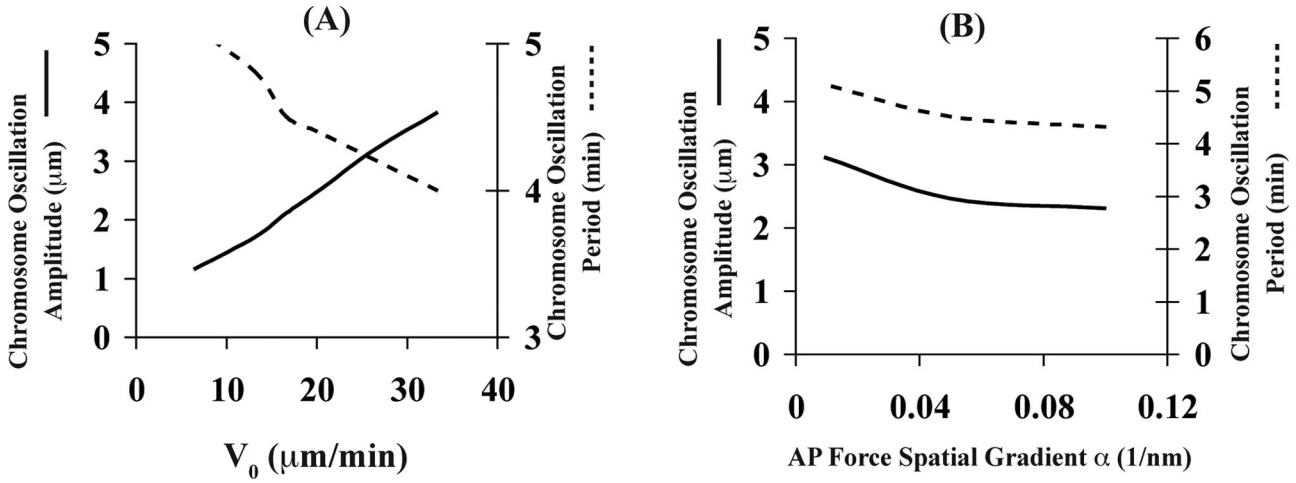

Fig. S3. (*A*) The dependence of bioriented chromosome oscillation on the velocity constant V_0. (*B*) The dependence of bioriented chromosome oscillation on the AP force spatial gradient α. If not otherwise mentioned, the parameters in the calculation are $k_1 = 0.1$ nM·min^{-1}, $k_2 = 0.06$ min^{-1}, $k_3 = 0.02$ nM^{-1}·min^{-1}, $k_4 = 0.25$ min^{-1}, $k_5 = 3.33$ min^{-1}, $k_6 = 3.33$ min^{-1}, $K_C = 0.2$ nM^{-1}, $V_0 = 20$ μm·min^{-1}, $|\alpha| = 0.01$ nm^{-1}, $l_0 = 1.0$ μm, $\tilde{K} = 0.001$, and the relative noise level $|\tilde{\xi}|/V_0 = 0.1$.

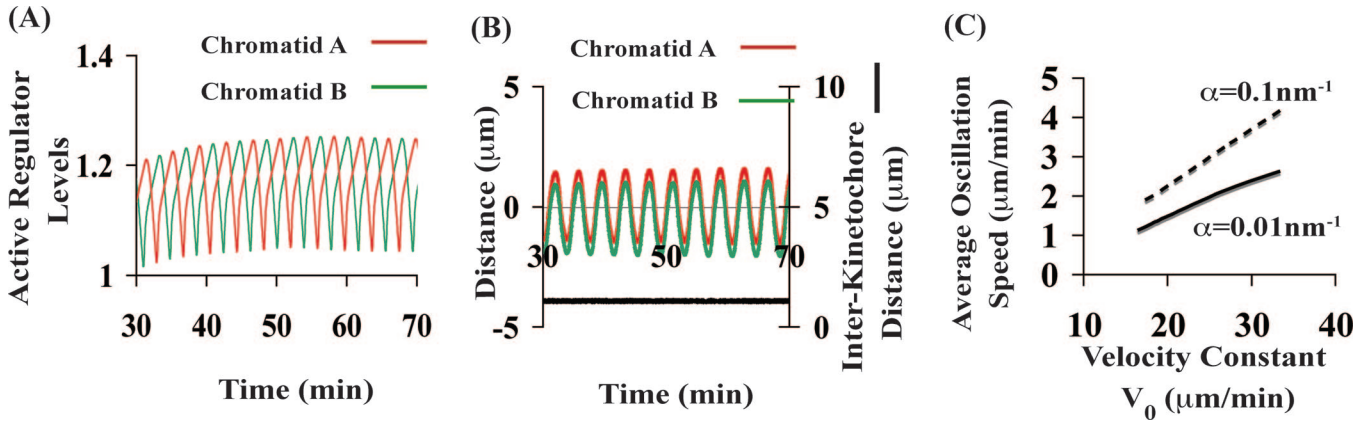

Fig. S4. (*A* and *B*) The chemical and mechanical states during oscillation for increased AP force spatial gradient α (α = 0.1 nm^{-1}) and velocity constant (V_0 = 33.3 μm/min). (*C*) The dependence of the average velocity of monooriented chromosome oscillation on the AP force spatial gradient α and the velocity constant V_0 (all of the parameters remain the same as in Fig. S3 except that there is no interaction between the sister chromatids (i.e., $\bar{K}$ = 0.001 and no steric repulsion). Thus, each sister chromatid acts as a monooriented chromosome).

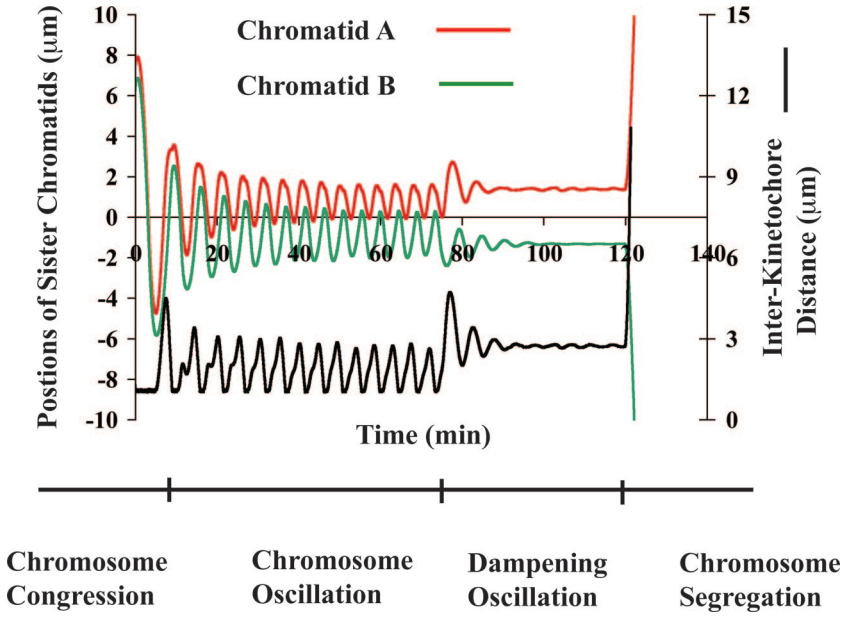

Fig. S5. The variation in the elastic constant of the cohesion between sister chromatids does not affect qualitative results from the model. With all of the other parameters remaining the same as in Fig. 2, $\bar{K}$ changes from 0.001 to 0.1. The most noticeable difference is that the interkinetochore distance after the dampening oscillation is a little bit smaller for the case of the stronger cohesion strength (changing from 3.1 μm in $\bar{K} = 0.001$ to 2.9 μm in $\bar{K} = 0.1$).

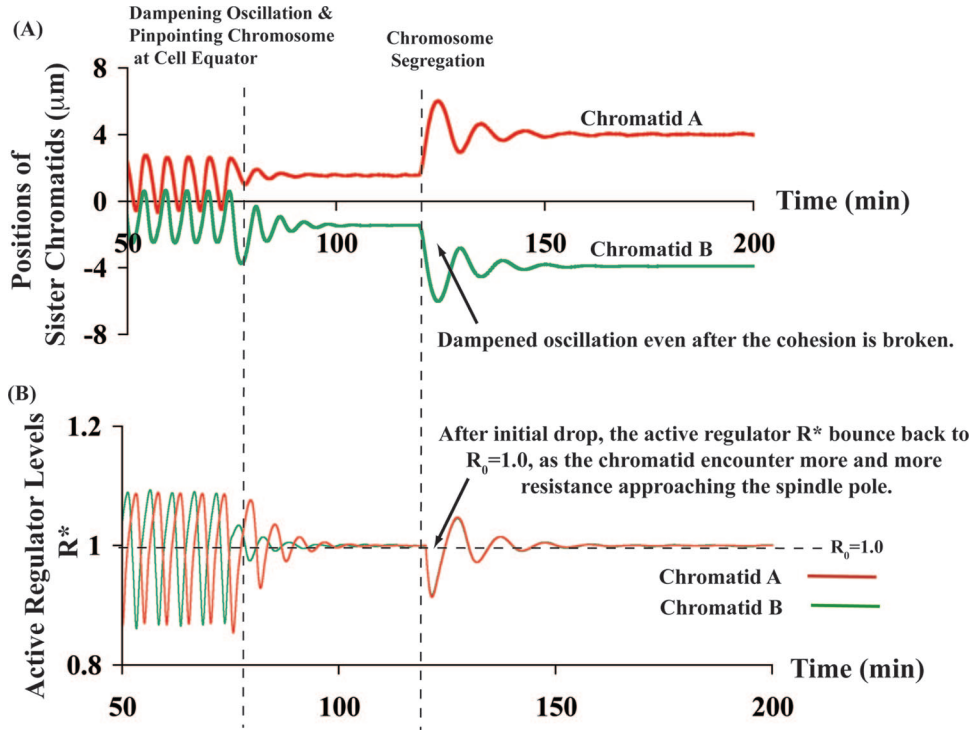

Fig. S6. After the sister chromatid segregates, it can still undergo dampened oscillation if the mechanobiochemical feedback is not completely disassembled: that is, the K_C in Fig. S4 remains at its initial value before chromosome segregation $K_C = 0.2\ \text{nM}^{-1}$, which is in comparison to the case in Fig. 2, where the feedback is totally depleted (K_C drops to zero) after the chromosome segregation, and segregated chromatids undergo sustained poleward movements.

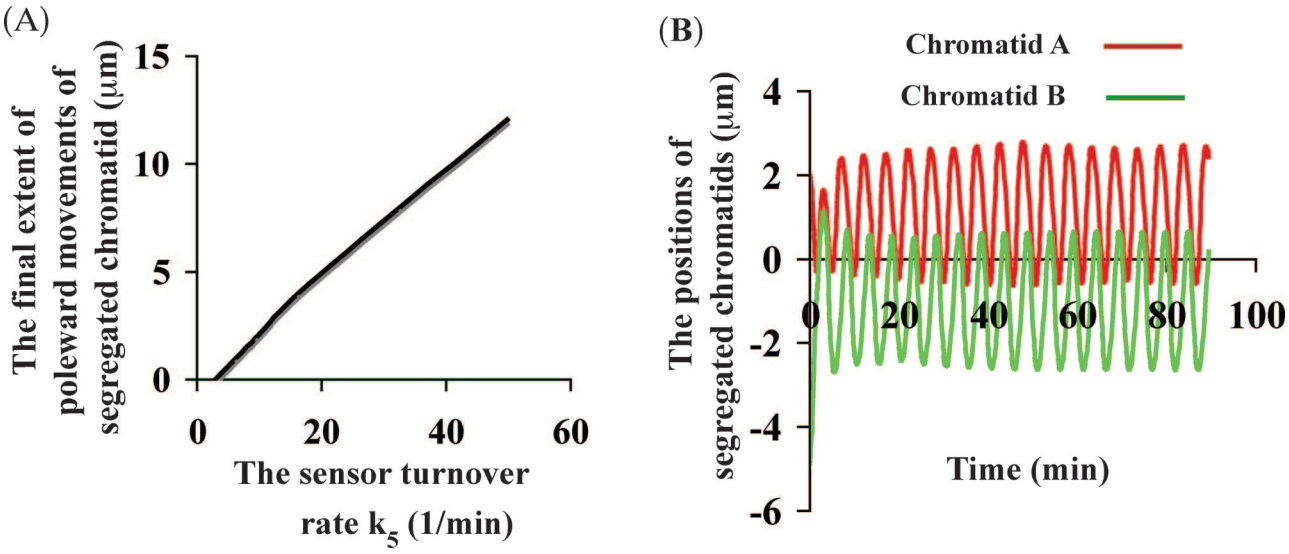

Fig. S7. (*A*) The extent of the poleward movement of segregated chromatids ($\bar{K} = 0$) depends on the turnover rate of the sensor protein k_5. The mechanobiochemical feedback is only partially impaired with K_C intact ($K_C = 0.2\ \mathrm{nM}^{-1}$). (*B*) Oscillation of the segregated chromatids. The localized feedback is fully maintained as the same condition of the bioriented chromosome oscillation shown in Fig. 2 in the main text.

Table S1. Kinetic parameters in the model

Symbol	Parameter	Value
k_1	Synthesis rate of R per kinetochore region	$\approx$0.1 nM·min^{-1} (1–5)
k_2	Bare activation rate of R	$\approx$0.05–0.07 min^{-1} (1–5)
k_3	Rate of R activation by S	$\approx$0.02 nM^{-1}·min^{-1} (1–5)
k_4	Bare rate of R degradation	$\approx$0.2–0.25 min^{-1} (1–5)
K_C	Equilibrium constant of Cdc20 and S conjugation	$\approx$(5 nM)$^{-1}$ (6–8)
k_5	Rate of S turnover	$\approx$2.0–3.0 min^{-1} (9, 10)
k_6	Response rate of S to force	$\approx k_5$ (estimated)
α	Effective AP force gradient	≈ -0.01 nm^{-1} (estimated)
$\bar{K}$	Elastic constant of the cohesion between sister chromatids	$\approx$0.001–1.0 (estimated)[†]
V_0	Chromosome velocity response rate after activation of R*, ensuring chromosome velocity $V < 5$ μm·min^{-1} (11)	
R_0	The threshold value, across which R* change chromosome movement direction	$\approx$1.0 (12)[‡]
l_0	The resting interkinetochore distance	$\approx$1.0–2.0 μm (13)

[†]It can be shown that the value of the elastic constant $\bar{K}$ does not qualitatively affect the characteristics of bioriented chromosome motility (see Fig. S5).

[‡]Because the typical amount of each protein at the kinetochore region is $\approx$500–5,000 molecules (12). We set R_0 to be 500 molecules; this value can be shown not to affect the behavior of the system. To simplify the description, we express the levels of all molecular species (Eqs. **1**-**4**) in the unit of R_0 and set it dimensionless (i.e., with $R_0 = 1$). It can be shown that this value does not affect the qualitative results.

1. Kumagai A, Dunphy WG (1995) Control of the Cdc2/cyclin B complex in *Xenopus* egg extracts arrested at a G_2/M checkpoint with DNA synthesis inhibitors. *Mol Biol Cell* 6:199–213.
2. Lee TH, Turck C, Kirschner MK (1994) Inhibition of cdc2 activation by INH/PP2A. *Mol Biol Cell* 5:323–338.
3. Breton ML, Cormier P, Bellé R, Mulne-Lorillon O, Morales J (2005) Translational control during mitosis. *Biochimie* 87:805–811.
4. Huang JY, Raff JW (1999) The disappearance of cyclin B at the end of mitosis is regulated spatially in *Drosophila* cells. *EMBO J* 18:2184–2195.
5. Huang JY, Raff JW (2002) The dynamic localization of the *Drosophila* APC/C: Evidence for the existence of multiple complexes that perform distinct functions and are differentially localized. *J Cell Sci* 115:2847–2856.
6. Sudakin V, Chan GKT, Yen TJ (2001) Checkpoint inhibition of the APC/C in HeLa cells is mediated by a complex of BUBR1, BUB3, CDC20, and MAD2. *J Cell Biol* 154:925–936.
7. Fang GW (2002) Checkpoint protein BubR1 acts synergistically with Mad2 to inhibit anaphase-promoting complex. *Mol Biol Cell* 13:755–766.
8. Tang ZY, Bharadwaj R, Li B, Yu HT (2001) Mad2-independent inhibition of APC^{Cdc20} by the mitotic checkpoint protein BubR1. *Dev Cell* 1:227–237.
9. Howell BJ, *et al*. (2004) Spindle checkpoint protein dynamics at kinetochores in living cells. *Curr Biol* 14:953–964.
10. Shah JV, *et al*. (2004) Dynamics of centromere and kinetochore proteins: implications for checkpoint signaling and silencing. *Curr Biol* 14:942–952.
11. Helenius J, Brouhard G, Kalaidzidis Y, Diez S, Howard J (2006) The depolymerizing kinesin MCAK uses lattice diffusion to rapidly target microtubule ends. *Nature* 441:115–119.
12. Emanuele MJ, McCleland ML, Satinover DL, Stukenberg PT (2005) Measuring the stoichiometry and physical interactions between components elucidates the architecture of the vertebrate kinetochore. *Mol Biol Cell* 16:4882–4892.
13. Kline-Smith SL, Khodjakov A, Hergert P, Walczak CE (2004) Depletion of centromeric MCAK leads to chromosome congression and segregation defects due to improper kinetochore attachments. *Mol Biol Cell* 15:1146–1159.